STScI | SPACE TELESCOPE SCIENCE INSTITUTE

Instrument Science Report STIS 2022-07 and ACS 2022-05

Typeset using LaTeX default style in AASTeX631

Update of the STIS CTE Correction Formula for Stellar Spectra

Ralph C. Bohlin and Sean Lockwood

ABSTRACT

The correction formula for Charge Transfer Efficiency (CTE) that is used in the HSTCAL CALSTIS pipeline CCD data reduction has not been significantly updated since 2006. Correcting for CTE losses is crucial to the goal of 1% precision in the STIS spectrophotometric fluxes that are the basis for all HST and JWST flux calibrations. Precision in the CTE correction is especially relevant for the faintest flux standards, where the amount of correction can exceed 20%. The comparison of new datasets of STIS spectra and ACS photometry of faint stars reveals the required updates to the parameters of the STIS CTE correction formula. After replacing the original with the new parameters, the change in the spectral energy distribution (SED), i.e. the flux decrease in physical units, for a very faint star NGC2506-G31 ranges from 4 to 6% over most of the G430L and G750L spectral wavelength ranges. No observations of the faint stars with G230LB or the medium dispersion modes were made; but the CTE correction depends only on signal level and should apply to all CCD spectroscopic modes. With the new formulation for the STIS CTE correction the STIS, ACS, and WFC3 flux measures are in accord at the 1% level, not only for the primary standards and other stars in the neighborhood of V=13 and brighter, but also now for fainter stars in the V=16 range.

Keywords: stars:fundamental parameters (absolute flux) — techniques:spectrophotometry, photometry — HST Instruments (ACS, STIS)

1. INTRODUCTION

The damage to the STIS CCD detector from cosmic-rays and trapped particle radiation in the Van Allen belts contributes to the loss of efficiency in the transfer of detected charge to the CCD readout amplifier. The preferred correction for these losses has been Goudfrooij et al. (2006a). Additional references are Bohlin (2003), Bohlin & Goudfrooij (2003), Goudfrooij et al. (2006b), Goudfrooij & Bohlin (2006), Biretta et al. (2015), and Prichard (2022). While the HSTCAL CALSTIS pipeline employs the Goudfrooij et al. (2006a) algorithm, there is also a pixel-based correction for CTE losses[1]. A future study will be devoted to a detailed comparison of the pixel-based correction for stellar spectra to the predictions of the revised Goudfrooij et al. (2006a) algorithm.

[1] https://www.stsci.edu/hst/instrumentation/stis/data-analysis-and-software-tools/pixel-based-cti

CTE losses are comonly known as Charge Transfer Inefficiency, CTI. The Goudfrooij et al. (2006a) model for CTI has withstood the test of time, but the formula requires some modification to its extrapolations from the data analyzed in 2005. Section 2 summarizes the recent observational programs for quantifying current CTE losses for spectra. Section 3 presents the analysis of these new data, and Section 4 illustrates the improvements to selected spectral energy distributions (SEDs).

2. NEW OBSERVATIONS

Because CTE losses (CTI) and losses from surface contamination both contribute to an overall sensitivity decline, disentangling the two contributions is problematic. The CTI depends on time in orbit, the location on the CCD chip with respect to the readout amplifier, the stellar signal strength, and the background level, while optical surface contamination generally just increases with time. Probably, the best way to derive the CTE correction is to analyze data obtained within a short interval of 2–3 years, so any change with time is minimal.

Cycle 28 programs 16514, 16515, and 16437 aim to quantify the CTI. Each observation is repeated three times to reduce noise from the faint signals that have the largest CTI and, therefore, the best constraints on the CTI correction formula. Short and long STIS exposures of the bright star BD+75°325 comprise 16515, while the STIS program 16437 observed faint stars that have the most CTI. The short exposures of BD+75°325 have little background signal, because STIS has no flash capability to produce typical sky levels. Matching the flux from the 16515 short and long exposures requires an increase of CTI with respect to the Goudfrooij et al. (2006a) baseline. On the other hand, the 16437 data with typical sky backgrounds of 5–20 electrons require a decrease in CTI to match the companion ACS 16514 photometry. This over-correction for CTI of the 16437 spectrophotometry with the Goudfrooij et al. (2006a) formula is consistent with the results of Prichard (2022) for STIS imaging photometry. A corollary is that the CTI correction formula presented in the next Section would produce a corrected flux that is too low when applied to an underexposured observation with weak signal and atypically low sky background. The analysis here concentrates on matching the STIS 16437 to the ACS 16514 data for four faint stars. The much smaller ACS CTE corrections are based on (Bohlin & Anderson 2011).

Table 1 summarizes the STIS (G430L & G750L) and the ACS (WFC1B-1K subarray) observations of faint stars obtained in ACS program 16514 and mostly in STIS program 16437. Three observations were made in each mode in order to achieve robust results. The observations are mostly within a two year epoch and approach the STIS faint limit to maximize CTI. Because the ACS and STIS flux calibrations are both derived from observations of the same three primary HST standards, G191B2B, GD153, and GD71, the measured absolute flux from ACS must agree with the synthetic flux from STIS spectra by definition for any star in the brightness range of the three primaries (V=11.8–13.3) (Bohlin 2016; Bohlin et al. 2020b). Any deviation from agreement for brighter or fainter stars must be attributed to errors in the linearity correction for either STIS or ACS. All ACS observations are subarrays with amp B readout, while all STIS data use the default D amp at the top right corner of the STIS CCD.

Table 1. Recent Observations of Faint Standards

Star	G (mag)	STIS Dates	ACS Dates	ACS Filters[a]
WDFS1514+00	15.88	2019Apr24 – 2021Sep15[b]	2021Jul26-2021Aug28	F550M
WD0308-565	14.10	2020Feb24 – 2022Jan29[c]	2021Aug26-2021Dec4	...
WD1057+719	14.70	2020Feb29 – 2021Dec22[c]	2021Sep15-2021Dec22	...
WD1657+343	16.42	2021Aug03 – 2021Sep16[d]	2021Jul26-2021Sep21	F550M,F850LP

[a] Filters missing from the set of F435W, F475W, F550M, F555W, F606W, F625W, F775W, F814W, F850LP

[b] Includes a G430L and a G750L 2019 observation from program 15487

[c] Includes a G430L and a G750L 2020 observation from program 16028

[d] Excluded from program 16028 are a noisy G430L spectrum with CR-split=1 and a G750L with individual CR-splits longer than the 10 min maximum limit.

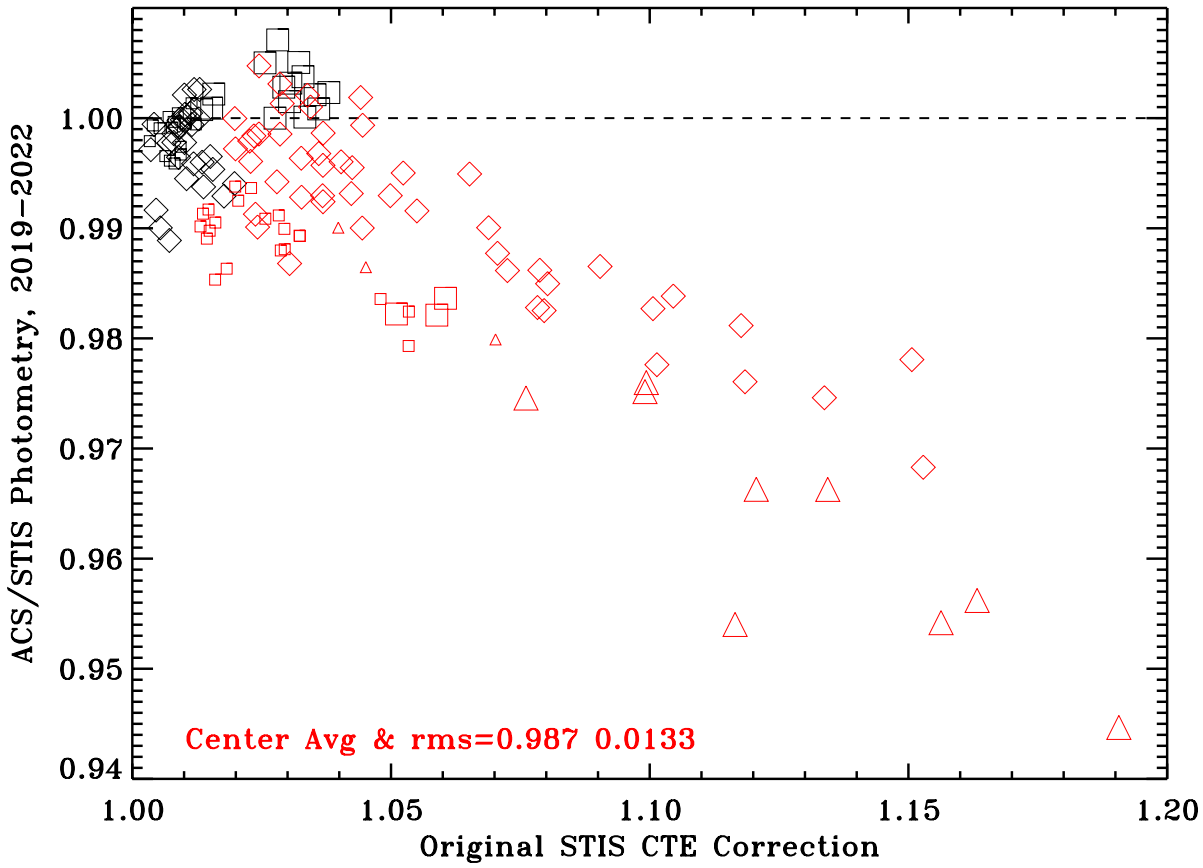

Figure 1. Ratio of average ACS photometry to individual synthetic photometry from STIS observations since 2019 of the bright stars G191B2B, GD153, and GD71 (black symbols) and for the faint stars WD0308-565, WD1057+719, WDFS1514+00 (SDSSJ151421.27+004752.8), and WD1657+343 (red symbols). The STIS data utilize the original CTE correction formula of Goudfrooij et al. (2006a). Triangles represent the faintest star WD1657+343 that has the largest CTE correction. Squares are for the shorter wavelength G430L covered mostly by the ACS filters F435W, F475W, F555W, F550M, while the diamond symbols are for F606W, F625W, F775W, F814W, F850LP where the synthetic photometry is mostly from the STIS G750L. Small squares are STIS G430L E1 data near the readout amp, where any change in the CTE formula has a much smaller effect than for spectra lying at CCD center. The diamonds and triangles with the largest STIS CTE correction (X-axis) are the filters at the longer wavelengths, where the STIS signal is the weakest and the CTE correction is the largest.

3. ANALYSIS

Figure 1 illustrates the poor extrapolation of the original Goudfrooij et al. (2006a) formula for a recent 2019-2022 epoch, where errors for the faint white dwarf star WD1657+343 (triangles) are ∼5% for the comparison of the STIS synthetic photometry with the actual ACS F814W filter photometry that overlaps the faintest region of the STIS signal. For example, the three STIS G750L observations of the faintest WD1657+343 compared to ACS in the F814W band are the three triangles with the largest CTE correction. The X-axis represents the average STIS CTE correction in the ACS bandpass, while the Y-axis is the ratio of each available STIS observation to the average of all ACS flux measurements in each filter since launch in 2002. The only ACS observations of the four faint stars (red) are in 2021–2022. The recent ACS flux calibration is documented by Bohlin et al. (2020b). The broadband agreement to ∼1% among such faint and noisy STIS spectra longward of ∼8000Å is at the expected, typical level.

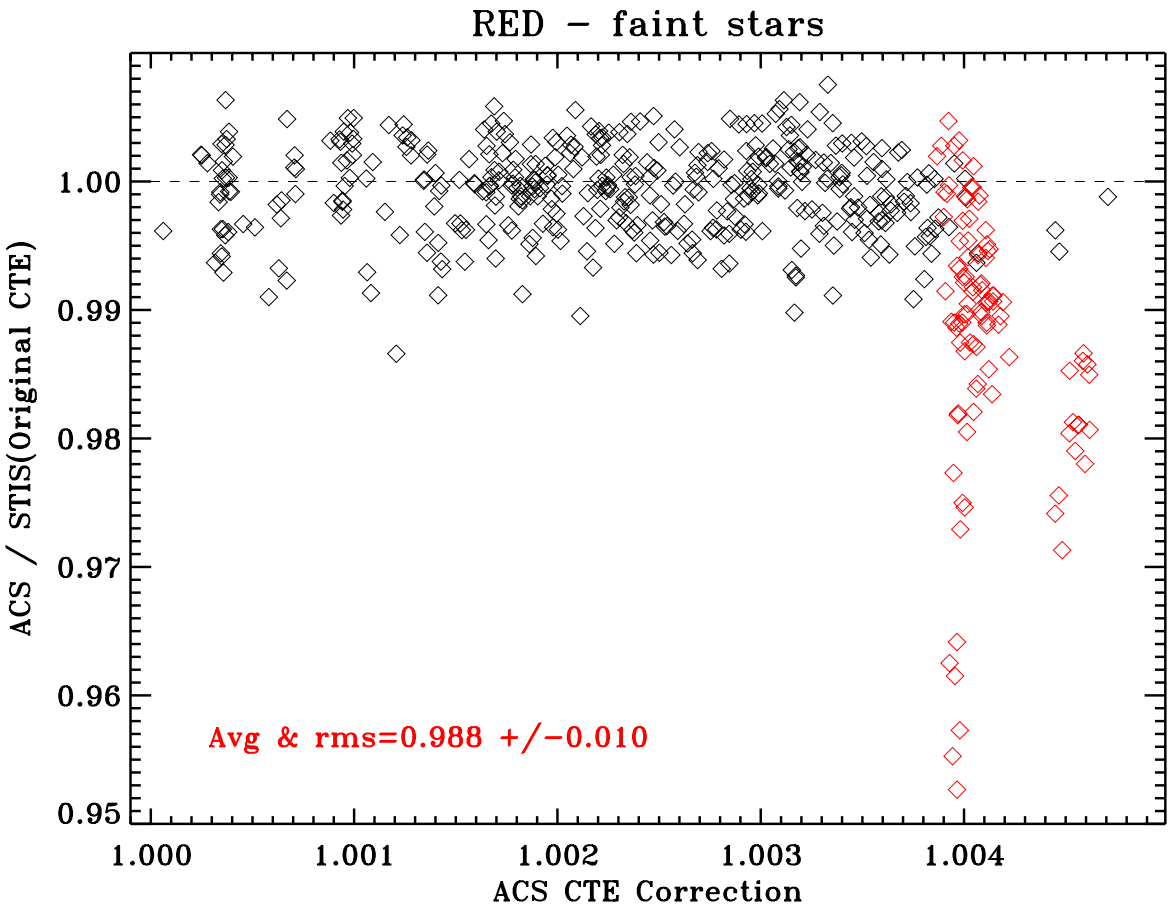

Figure 2. Ratio of ACS photometry to STIS synthetic photometry as in Figure 1, except for each ACS photometry point vs. the average STIS SED. The X-axis is now the ACS CTI, instead of the much larger STIS CTI. Data points for the three primary WDs are black, while red represents the four faint stars.

Figure 2 shows a similar comparison for each ACS photometry data point divided by the STIS synthetic photometry from the average STIS SED. The range in the Y-axis ratios is similar to Figure 1, but the X-axis now shows the much smaller ACS CTE correction, which is a parameterization of the ACS pixel-based CTE correction (Bohlin & Anderson 2011). This parameterization reduces the excess noise introduced by the pixel-based correction and eliminates the special ACS_DESTRIPE_PLUS processing step that corrects subarrays for CTE losses. The three ACS correction techniques, ACS_DESTRIPE_PLUS, Bohlin & Anderson (2011), and Chiaberge (2012) provide consistent results (Bohlin et al. 2020b). The faint stars for STIS spectrophotometry are still bright for ACS photometry, so all of the ACS exposures are near optimal and have nearly the same CTI. The spread in CTE correction from 1.000 to 1.005 for the four standard stars G191B2B, GD153, GD71, and GRW+70°5824 (black diamonds) is due to including all of their exposures since launch in 2002, while the four fainter stars (red) of Table 1 are all from the narrow epoch of 2021-2022. Even if the ACS correction were in error by as much as a factor of two, that error of <0.5% would not make a big change in the STIS errors illustrated in Figure 1. Thus, an excellent first order update to the STIS CTI correction formula results from minimizing the errors appearing in Figure 1.

Assuming the current ACS CTI correction is perfect, Figure 3 is the result of finding new parameters to minimize the Figure 1 errors. Most data points in Figure 3 fall within 1% of unity and only one point shows more than a 2% error. The average ACS/STIS flux ratio for all 61 red faint-star points that lie at the CCD center row is within 0.1% of an optimal new STIS CTI correction compared to the average error of the current formula of 1.3% shown as the average ratio of 0.987 in Figure 1; and the only 3σ residual drops from 5.5% to 2%.

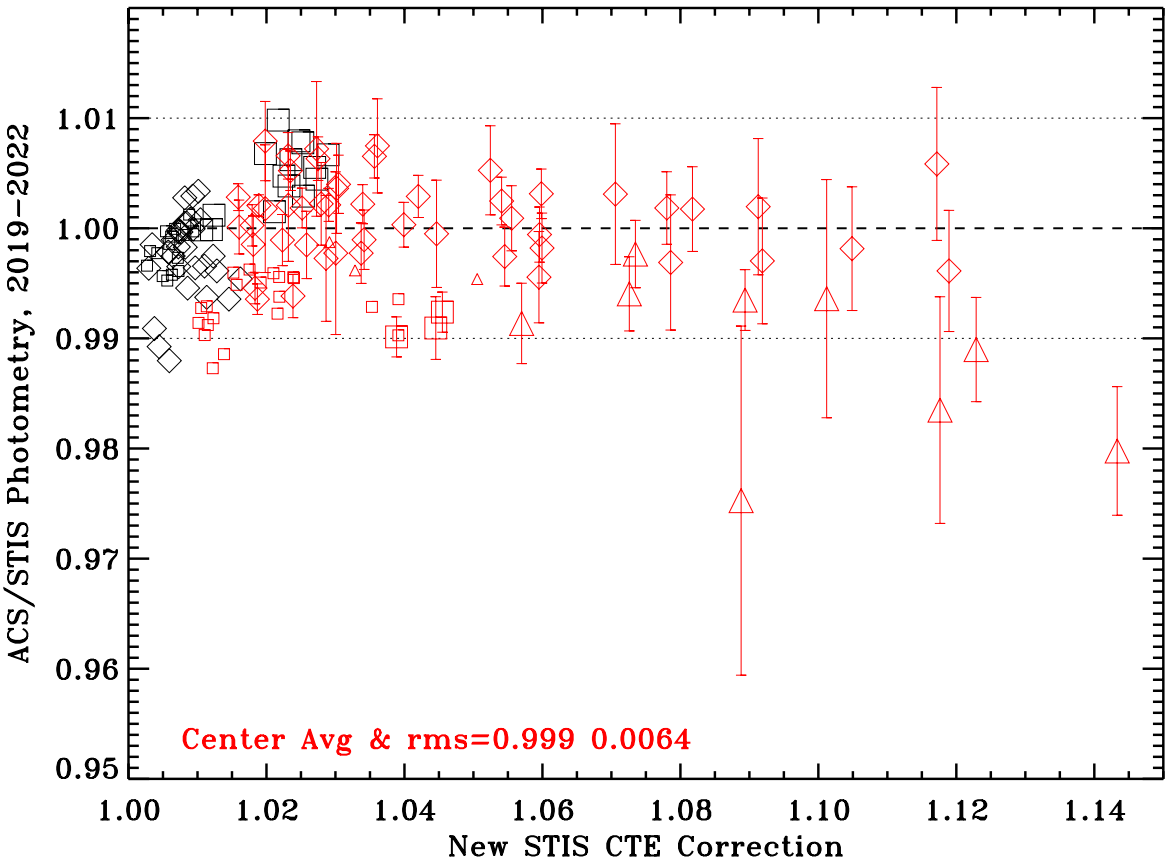

Figure 3. Ratio of ACS photometry to STIS synthetic photometry as in Figure 1, except for the newly updated STIS CTE correction. Dotted lines delineate the region where ACS and STIS agree within 1%; and error bars are one sigma.

Table 2. Parameters of STIS CTI for Equation 1

Param.	Value	Description
α	0.0562	CTI normalization
β	0.82	Gross count-level dependence
γ	0.216[a]	Time dependence
δ	3.4 (3.0)	Factor for Total–background/Gross
ϵ	0.8 (1.3)	Factor for G750L halo
ζ	0.16 (0.18)	Power for background/Gross
η	0.06	Minimum of G750L halo fraction

[a]Updated by Goudfrooij et al. (2009)

Table 2 has the revised parameters of the Goudfrooij et al. (2006a) CTI correction formula where the three updated values also have the original values in parentheses. There is no evidence that any of the seven parameters changes with time; and some, e.g. γ, is derived independently from the annual internal sparse field data (Goudfrooij et al. 2009). According to the uncertainty estimates σ of Goudfrooij et al. (2006a), our updates in units of σ for δ, ϵ, and ζ are 8,

5, and 2, respectively. The formula is

$$CTI = \alpha G^{-\beta}\ [\gamma(t - 2000.6) + 1]\ exp\left[-\delta\left(\frac{B' + \epsilon H'}{G}\right)^{\zeta}\right], \quad (1)$$

where G is the wavelength-dependent gross signal in detected electrons for the 11 pixel extraction height (Bohlin & Proffitt 2015; Bohlin et al. 2019)[2] before subtracting the sky background B to get the net signal, t is the decimal time of year of the observation, B' is the sum of B plus the dark current plus the spurious charge in STIS bias frames, and H' accounts for the G750L extra background signal from scattering of long wavelength photons in the CCD mounting substrate, i.e. H'=[(H-η) $>$ 0] $\times$ net. G includes the dark current plus the spurious charge. H as a function of wavelength is derived from existing CALSTIS photometric correction tables (PCTAB) that define the fraction of PSF signal between the default 11 pixel extraction width and the readout amplifier (Goudfrooij & Bohlin 2006). These *_pct.fits tables appear in the PCTAB keyword of the STIS data headers. H'=0, except for the long wavelength G750L and G750M modes. The dark current is specified by the keyword MEANDARK divided by the number of co-added exposures, while the spurious charge is from the SPURCHARGE column of the CCDTAB reference table. For clarity, the sky background is electrons per pixel as a function wavelength and is just B and *not* the background (11 $\times$ B) that is subtracted from the gross signal G in the 11 pixel extraction width to get the net=G-11B. The quantities G, B, and H that characterize the extracted STIS spectrum apply to the individual exposures of a dithered or CR-split observation, *not* to the final sum of signal tabulated in the archival STIS *sx1.fits files. The quantity B is the smoothed version of the extracted sky signal. While the STIS spectra used in Figure 3 for the derivation of the three revised parameters of Table 2 are all unbinned at gain=1, the new values should also apply to gain=4 and binned data. The Goudfrooij et al. (2006a) version of our Equation 1 incorporates the rare useage of binning.

The new values result from analysis of stellar spectra extracted with the photometric height of 11 pixels (Bohlin & Proffitt 2015; Bohlin et al. 2019), rather than the STIS Archival products that are for a seven pixel height. The background B is from regions with a constant signal vs. row and should need no CTE correction; and there should be little error in correcting Archival *sx1,fits files with the revised parameters, because the gross signals G differs by only a few percent between seven and eleven pixel extractions. However, to fully implement any change in the CTE correction, the time and temperature reference files along with those for absolute flux sensitivity must all be updated using the net signals as corrected with the revised δ, ϵ, and ζ.

Because Equation 1 represents the CTI per row of charge transfer in the CCD readout, the total efficiency is

$$(1 - CTI)^{(1024 - row)}\ , \quad (2)$$

where row=1 at the bottom of the CCD and row=1024 at the top. To produce the corrected gross, divide the measured gross signal G by the efficiency of Equation 2.

4. STELLAR FLUX CHANGES

Figure 4 shows the change in flux of six stars that cover the brightness range of the HST CALSPEC[3] flux standards. The flux of the three primary WD flux standards, e.g. GD153 in purple, do not change on average, because the whole combined flux calibration scheme including the CTI correction, the time dependent sensitivity correction, the temperature correction, and flux calibration itself must reproduce the established flux of these three stars on average (Bohlin et al. 2020a). While the reduced CTI correction does reduce the flux of fainter stars, the SEDs of the brighter stars, e.g. Sirius that has zero CTI correction, must increase by the small amount of the average change of the CTI correction for the three primary WDs that range in V from 11.78 to 13.35. Stars that are fainter than WD0308-556 change by more than 1% and, obviously, did not previously meet the goal of a 1% flux accuracy. However, Figure 3 suggests that the revised CTI correction brings the updated SEDs much closer to the goal of 1% accuracy in absolute flux for such faint stars.

[2] Archival CALSTIS spectra utilize a 7 pixel extraction height to slightly improve S/N for faint stars, instead of optimizing photometric precision with a height of 11 pixels.

[3] https://www.stsci.edu/hst/instrumentation/reference-data-for-calibration-and-tools/astronomical-catalogs/calspec

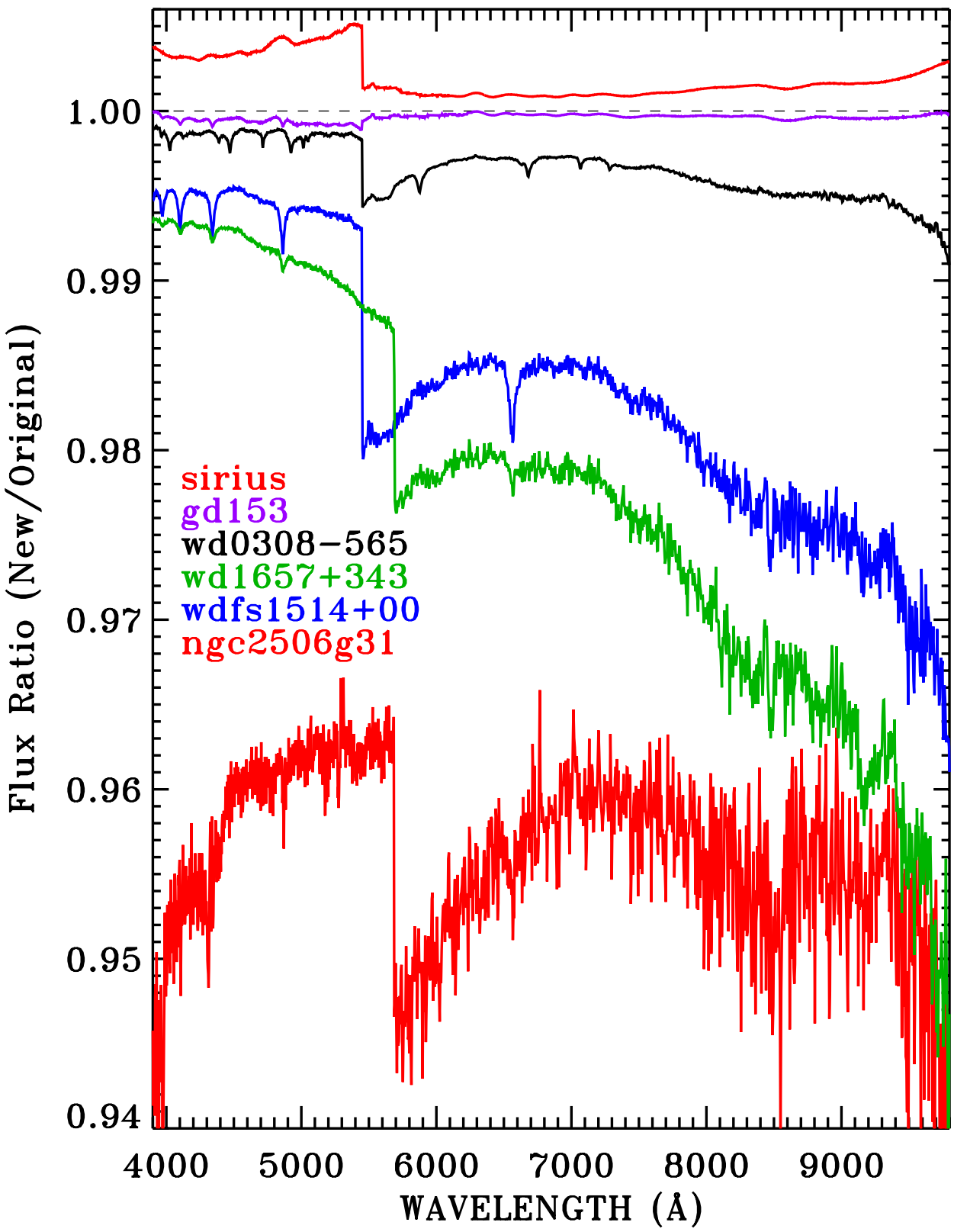

Figure 4. Ratio of stellar SEDs derived for the updated CTE correction divided by the SED found using the original formula of Goudfrooij et al. (2006a). The range of brightness covers the faintest (NGC2506-31, V=17.9) to the brightest (Sirius, V=-1.46) CALSPEC star.

For isolated cases, there are regions of CALSPEC SEDs where the updated flux drops by even more than for the stars in Figure 4. The cool L3.5 CALSPEC standard 2M003618 (2MASS J00361617+1821104) has a count rate that falls to ∼0.01 electrons/s in its faint region. The corresponding total electron level is ∼50 electrons in each spectrum of the CR-split. The revised flux at 5840-5890 Å is 25% less than with the Goudfrooij et al. (2006a) formula, as illustrated in Figure 5. This 25% over-correction of the original CTI correction is much larger than the typical over-corrections in Figure 1, because the signal of 50 electrons is much lower than any signal in the STIS spectra used to construct Figure 1. Over half of the CALSPEC SEDs have substantial changes of >0.5% and must be re-delivered.

Figure 6 is a good example of a benefit of the updated CTI correction, which shows that the revised formulation improves the agreement of the faint and relatively noisy STIS SED of WDFS1514+00 with its model SED that is based on the WFC3 photometric flux calibration. The model results from a fitting of the WFC3 photometry with a pure hydrogen WD grid by Axelrod et al. (2023, in prep.), and the program is a continuation and expansion of the Narayan et al. (2019) set of faint DA WD spectrophotometric standards from HST programs 12967, 13711, and 15113. While Axelrod uses the old Calamida et al. (2019) WFC3 flux calibration that is based on the old primary standards that differ from the current STIS primary standards of Bohlin et al. (2020b) by ∼2% on average over the STIS wavelength range, the model fluxes of Figure 6 are corrected to the current WFC3 flux scale of Calamida et al. (2022). With the revised CTI correction (red line and squares), the average agreement is improved by 2% and the rms difference between the model and STIS SEDs is cut from 2% to 1%. While Figure 3 demonstrates the improved agreement of the updated STIS fluxes with the current ACS flux calibration, Figure 6 demonstrates an additional sub-percent agreement with the WFC3 flux calibration for faint stars.

5. RECOMMENDATIONS

Early observations of WD1657+343 would have provided the best constraints on the CTI correction algorithm, but adding a faint flux standard like WD1657+343 to the STIS annual monitoring of the bright star AKG+81°266 would be beneficial to future STIS CTI update efforts. Any changes with time in the fully corrected WD1657+343 flux distribution must be attributed to errors in the non-linear CTI correction. Now that the G230L flux from NUV MAMA data is well established, future G230LB observations of the faint standards could also help monitor and refine the CTI correction formula. G230LB observations of the faint WD1657+343 could have been included in the STIS program 16437 at the expense of three additional orbits.

6. ACKNOWLEDGEMENTS

Annalisa Calamida, Svea Hernandez, and Jenna Ryon provided suggestions and comments that improved this ISR. Support for this work was provided by NASA through the Space Telescope Science Institute, which is operated by AURA, Inc., under NASA contract NAS5-26555. This research has made use of the SIMBAD database, operated at CDS, Strasbourg, France.

ORCID IDs

Ralph C. Bohlin https://orcid.org/0000-0001-9806-0551

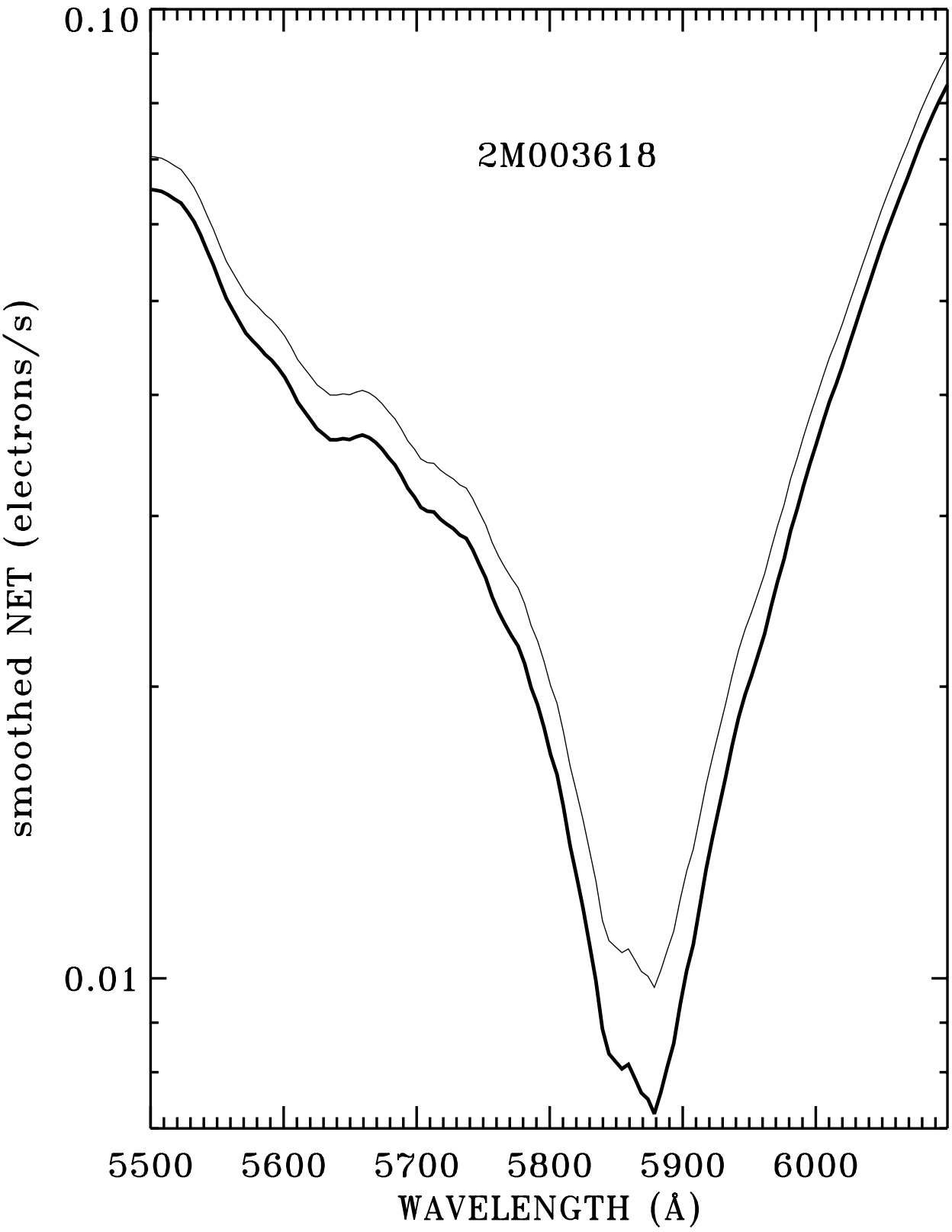

Figure 5. Net count rate for 2M003618 as corrected with the Goudfrooij et al. (2006a) formula (thin) and with the new parameters (thick).

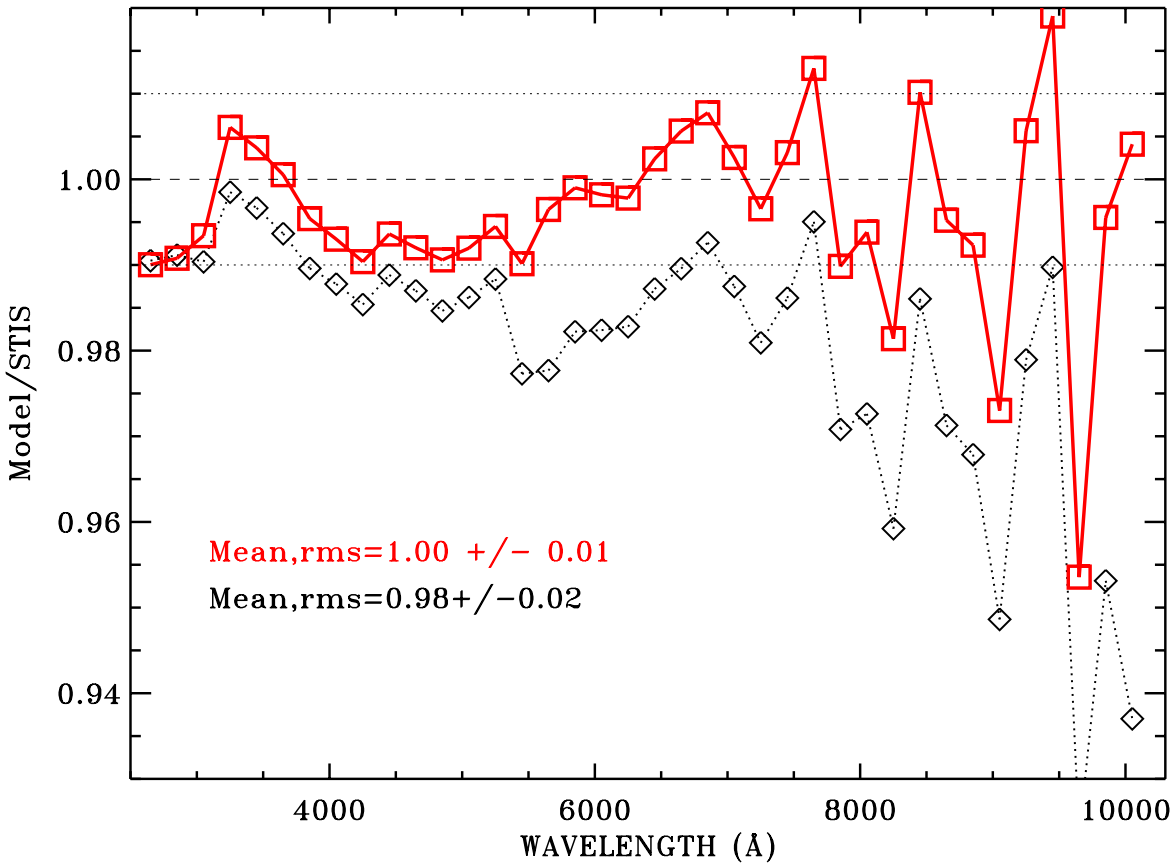

Figure 6. Ratio of the pure hydrogen model for WDFS1514+00 to the STIS SED in 200 Å bins. Black diamonds represent the STIS data as corrected with the Goudfrooij et al. (2006a) formula, while the red squares are results from the updated formula.

REFERENCES

Biretta, J., Lockwood, S., & Debes, J. 2015, STIS CCD CTI Column Temperature Dependence, Tech. rep.

Bohlin, R., & Goudfrooij, P. 2003, An Algorithm for Correcting CTE Loss in Spectrophotometry of Point Sources with the STIS CCD, STIS ISR 2003–03R, Tech. rep.

Bohlin, R. C. 2003, in HST Calibration Workshop : Hubble after the Installation of the ACS and the NICMOS Cooling System, 115

Bohlin, R. C. 2016, AJ, 152, 60

Bohlin, R. C., & Anderson, J. 2011, Flux Calibration of the ACS CCD Cameras I. CTE Correction, Instrument Science Report, ACS 2011–01, (Baltimore: STScI), Tech. rep.

Bohlin, R. C., Deustua, S. E., & de Rosa, G. 2019, The Astronomical Journal, 158, 211

Bohlin, R. C., Hubeny, I., & Rauch, T. 2020a, AJ, 160, 21

Bohlin, R. C., & Proffitt, C. R. 2015, Improved Photometry for G750L, Instrument Science Report, STIS 2015–01, (Baltimore: STScI), Tech. rep.

Bohlin, R. C., Ryon, J. E., & Anderson, J. 2020b, Update of the Photometric Calibration of the ACS CCD Cameras, Instrument Science Report ACS 2020-8

Calamida, A., Matheson, T., Saha, A., et al. 2019, ApJ, 872, 199

Calamida, A., Bajaj, V., Mack, J., et al. 2022, AJ, 164, 32

Chiaberge, M. 2012, A new accurate CTE photometric correction formula for ACS/WFC, Instrument Science Report, ACS 2012–05, (Baltimore: STScI), Tech. rep.

Goudfrooij, P., & Bohlin, R. C. 2006, A new CTE Correction Algorithm for Point Source Spectroscopy with the STIS CCD: Correcting for charge trap filling by the red halo of the CCD Point Spread Function redward of 8000 Å, STIS ISR 2006-03, Tech. rep.

Goudfrooij, P., Bohlin, R. C., Maíz-Apellániz, J., & Kimble, R. A. 2006a, PASP, 118, 1455

Goudfrooij, P., Maíz Apellániz, J., Brown, T., & Kimble, R. 2006b, Charge Transfer Efficiency of the STIS CCD:The time dependence of charge loss and centroid shifts from Internal Sparse Field data, STIS ISR 2006-01, Tech. rep.

Goudfrooij, P., Wolfe, M. A., Bohlin, R. C., Proffitt, C., & Lennon, D. J. 2009, STIS CCD Performance after SM4: Read Noise, Dark Current, Hot Pixel Annealing, CTE, Gain, and Spectroscopic Sensitivity, STIS ISR 2009-02, Tech. rep.

Narayan, G., Matheson, T., Saha, A., et al. 2019, ApJS, 241, 20

Prichard, L. 2022, Comparison of STIS CCD CTI Corrections on Photometry, Tech. rep.